The Journal of Immunology

Epithelial Control of Gut-Associated Lymphoid Tissue Formation through p38 α -Dependent Restraint of NF-κB Signaling

Celia Caballero-Franco, Monica Guma, Min-Kyung Choo, Yasuyo Sano, Thomas Enzler, Michael Karin, Atsushi Mizoguchi and Jin Mo Park

J Immunol 2016; 196:2368-2376; Prepublished online 20 January 2016;
doi: 10.4049/jimmunol.1501724
http://www.jimmunol.org/content/196/5/2368

The Journal of Immunology is published twice each month by
The American Association of Immunologists, Inc.,
1451 Rockville Pike, Suite 650, Rockville, MD 20852

Print ISSN: 0022-1767 Online ISSN: 1550-6606.

Epithelial Control of Gut-Associated Lymphoid Tissue Formation through p38α-Dependent Restraint of NF-κB Signaling

Celia Caballero-Franco,* Monica Guma,[†,‡] Min-Kyung Choo,* Yasuyo Sano,* Thomas Enzler,[*,§] Michael Karin,[†,¶] Atsushi Mizoguchi,[‖] and Jin Mo Park*

The protein kinase p38α mediates cellular responses to environmental and endogenous cues that direct tissue homeostasis and immune responses. Studies of mice lacking p38α in several different cell types have demonstrated that p38α signaling is essential to maintaining the proliferation–differentiation balance in developing and steady-state tissues. The mechanisms underlying these roles involve cell-autonomous control of signaling and gene expression by p38α. In this study, we show that p38α regulates gut-associated lymphoid tissue (GALT) formation in a noncell-autonomous manner. From an investigation of mice with intestinal epithelial cell-specific deletion of the p38α gene, we find that p38α serves to limit NF-κB signaling and thereby attenuate GALT-promoting chemokine expression in the intestinal epithelium. Loss of this regulation results in GALT hyperplasia and, in some animals, mucosa-associated B cell lymphoma. These anomalies occur independently of luminal microbial stimuli and are most likely driven by direct epithelial–lymphoid interactions. Our study illustrates a novel p38α-dependent mechanism preventing excessive generation of epithelial-derived signals that drive lymphoid tissue overgrowth and malignancy. ***The Journal of Immunology*****, 2016, 196: 2368–2376.**

The kinase p38 serves signaling functions that are conserved in a wide range of eukaryotic species—from single-celled fungi to mammals (1). In all organisms possessing its homologs, p38 is activated by various forms of environmental stress and signals to deploy appropriate cellular coping mechanisms. Besides its role in the cell-autonomous stress response, p38 functions downstream of receptors for cell-extrinsic signals that direct coordinated cell activities in multicellular organisms. Conversely, p38 also functions upstream of such receptors by modulating the production of their ligands. Receptor-mediated cell-to-cell communication that entails p38 signaling as an intracellular module is a theme prominent in the context of the immune response as well as tissue development and homeostasis. Among the four mammalian p38 isoforms, p38α is the most widely expressed in tissues and has established connections with diverse signaling receptors for microbial products, cytokines, growth factors, and hormones (2). By examining the effects of p38α gene ablation in mice, several studies including ours have revealed a role for p38α in tissue homeostasis, inflammation, and tumorigenesis (3). In parenchymal cells of various tissues, p38α signaling limits proliferation while promoting differentiation and survival (4–9). Hence, loss of p38α signaling in hepatocytes, keratinocytes, and intestinal epithelial cells (IECs) leaves them prone to damage and neoplastic transformation upon exposure to chemical irritants or carcinogens. It remains unclear, however, whether p38α signaling in parenchymal cells also performs noncell-autonomous functions, influencing the formation and maintenance of the stromal and hematopoietic-derived compartments of the tissue.

The intestinal mucosa provides vital physiological functions such as permeability barrier, nutrient transport, and neuroendocrine control. This versatility is mainly attributable to the functional capabilities and genetic program intrinsic to the mucosal epithelial compartment. IECs are also pivotal to orchestrating immune defense against pathogens and establishing tolerance to innocuous commensal microbes and dietary proteins. Lymphocytes and other hematopoietic-derived cells, highly abundant in intestinal tissues, also contribute to immunity and tolerance by furnishing effector and regulatory mechanisms that complement those conferred by IECs. Although T cells and plasma cells are found diffusely in the lamina propria, the vast majority of intestinal B cells are located within follicular structures. Several distinct types of lymphoid structures—collectively termed gut-associated lymphoid tissue (GALT)—are present in mammalian intestines (10, 11). Some of these structures develop prenatally under genetically programmed guidance, as exemplified by Peyer's patches in the ileum and the mesenteric lymph nodes. RORγ*t*-expressing lymphoid tissue inducer (LTi) cells are essential to this developmental process. Other forms of GALT, such as isolated lymphoid follicles (ILFs), develop postnatally. ILFs are discrete B cell aggregates scattered

*Cutaneous Biology Research Center, Massachusetts General Hospital and Harvard Medical School, Charlestown, MA 02129; [†]Department of Pharmacology, Laboratory of Gene Regulation and Signal Transduction, School of Medicine, University of California, San Diego, La Jolla, CA 92093; [‡]Division of Rheumatology, Allergy, and Immunology, School of Medicine, University of California, San Diego, La Jolla, CA 92093; [§]Department of Medicine, University of Arizona Cancer Center, Tucson, AZ 85724; [¶]Department of Pathology, School of Medicine, University of California, San Diego, La Jolla, CA 92093; and [‖]Department of Pathology, Molecular Pathology Unit, Massachusetts General Hospital and Harvard Medical School, Charlestown, MA 02129

ORCIDs: 0000-0003-1492-7539 (M.-K.C.); 0000-0001-9838-9357 (T.E.).

Received for publication July 31, 2015. Accepted for publication December 18, 2015.

This work was supported by National Institutes of Health Grants AI074957 (to J.M.P.) and AI043477 (to M.K.).

Address correspondence and reprint requests to Dr. Jin Mo Park, Cutaneous Biology Research Center, Massachusetts General Hospital and Harvard Medical School, 149 Thirteenth Street, Charlestown, MA 02129. E-mail address: jmpark@cbrc2.mgh.harvard.edu

The online version of this article contains supplemental material.

Abbreviations used in this article: DSS, dextran sulfate sodium; GALT, gut-associated lymphoid tissue; IEC, intestinal epithelial cell; ILF, isolated lymphoid follicle; KD, knockdown; LTi, lymphoid tissue inducer; shRNA, short hairpin RNA; siRNA, small interfering RNA; WT, wild-type.

across the small intestine and the colon, and contain T cells and other hematopoietic-derived cell types as minor constituents. ILF development is not only genetically programmed, but also conditioned by environmental inputs such as luminal microbial stimulation, and proceeds in two phases: the formation of RORγt$^+$ LTi-like cell clusters known as cryptopatches, and subsequent recruitment of B cells to cryptopatches for follicle growth. The GALT thus formed participates in local immune defense as well as shaping the systemic B cell repertoire. GALT-mediated immunity is phylogenetically more recent relative to epithelial-intrinsic defense mechanisms, and most likely evolved concomitantly with epithelial-derived signals that direct GALT development.

In this study, we discover a novel mechanism that mediates epithelial–lymphoid interactions in the intestinal mucosa: p38α functions to attenuate NF-κB target gene expression in IECs and thereby limits epithelial-derived signals driving GALT formation and malignancy. Our findings illustrate a critical role for the intestinal epithelium in GALT homeostasis, and point to p38α signaling as a key regulatory module in this process.

Materials and Methods

Animals

The mouse lines p38αΔIEC (*Mapk14$^{fl/fl}$-VilCre*) and IEC-IKKβ^{EE} (transgenic Vil-IKKβ^{EE}) were previously described (8, 12). RAG1-knockout mice (Rag1^{tm1Mom}) were obtained from The Jackson Laboratory. All mice were on a C57BL/6 background and maintained in a specific pathogen-free condition. To suppress establishment of the intestinal microbiota, mice were administered a mixture of the following antibiotics in drinking water: ampicillin (1 g/L), neomycin sulfate (1 g/L), vancomycin (0.5 g/L), and metronidazole (1 g/L; all from Sigma-Aldrich). Treatment with antibiotics began in utero by providing antibiotics to the mothers as soon as the mating cages were set up, and continued postnatally until the mice were sacrificed for analysis. To induce colitis, mice were administered 2.5 or 3.5% dextran sulfate sodium (DSS) in drinking water for 7 d; afterward, drinking water without DSS was provided. Survival was monitored daily over a period of 14 d. All animal experiments were conducted under Institutional Animal Care and Use Committee–approved protocols.

Cell lines and cell culture

MODE-K mouse IECs (13) were cultured in DMEM with high glucose (Life Technologies) supplemented with FBS (10%), penicillin (50 U/ml), and streptomycin (50 μg/ml). To enrich cells expressing the puromycin resistance gene, puromycin (2 μg/ml; EMD Millipore) was added to culture medium 36 h after plasmid DNA transfection. Cells were analyzed after 48 h of puromycin selection.

Reagents

Cultured cells were treated with mouse rTNF (a gift of C. Libert, Ghent University) and the TAK1 inhibitor (5Z)-7-oxozeaenol (Sigma-Aldrich). The RNAi Consortium plasmids expressing p38α-specific short hairpin RNA (shRNA; Dharmacon; Supplemental Table I) were in the pLKO.1 vector. RelA- and p38α-specific small interfering RNA (siRNA) was from the Stealth RNAi collection (Life Technologies; Supplemental Table I). Cell transfection with plasmid DNA and siRNA was performed using FuGENE HD (Roche) and Lipofectamine RNAiMAX (Life Technologies) transfection reagents, respectively. Flow cytometry was performed using fluorescent dye-conjugated Abs against the following markers: B220 (RA3-6B2) and CD3e (145-2C11; both from eBioscience). Immunostaining of tissue sections and bone marrow smears was performed with Abs against the following markers: B220 (RA3-6B2), CD4 (RM4-5), and CD11c (HL3; all from BD Biosciences); CD3e (SP7; Abcam); RORγt (B2D; eBioscience); and RelA (sc-372; Santa Cruz Biotechnology). For detection of germinal centers, tissue sections were stained with biotin-conjugated peanut agglutinin (Sigma-Aldrich). Immunoblotting was performed using Abs against the following proteins: RelA (sc-372), p38α (sc-535), AKT1/2/3 (sc-8312), and BRG1 (sc-10768; all from Santa Cruz Biotechnology); p38β (33-8700; Life Technologies); and p38γ and p38δ (gifts of S. Arthur, University of Dundee).

Lymphocyte isolation and flow cytometry

Lymphocytes were isolated from mouse colons and Peyer's patches, as described (14). Single-cell suspensions thus prepared were incubated with Fc receptor-blocking anti-CD16/CD32, stained with fluorescent-conjugated Abs, and analyzed by flow cytometry using FACSCanto (BD Biosciences) and FlowJo software (Tree Star).

Histology and immunofluorescence

Mouse ileum and colon samples were frozen in OCT medium or formalin fixed and embedded in paraffin. Sections of 5–7 μm in thickness on slides were stained with H&E or incubated with marker-specific primary Abs. Bone marrow smears on slides were air dried, fixed in methanol, and stained with Wright-Giemsa dyes (Sigma-Aldrich) or incubated with marker-specific Abs. For fluorescence labeling, the tissue sections and smears were incubated with secondary Abs conjugated with Alexa Fluor 488 or Alexa Fluor 594 or with streptavidin conjugated with Alexa Fluor 594 (Molecular Probes) and counterstained with Hoechst 33342 (Molecular Probes). Immunostained samples were analyzed by fluorescence microscopy.

Analysis of fecal bacteria

Fecal pellets were collected from mice, disintegrated and serially diluted in PBS, and plated on Luria-Bertani agar plates. Colonies were counted after 16 h of incubation at 37°C.

Analysis of Ig gene rearrangement

DNA from lymphomas and splenic B cells was analyzed by PCR using degenerate primers specific to different products of V_H-DJ_H rearrangement (15).

Protein and RNA analysis

Whole-cell lysates and extracts of cytoplasmic and nuclear fractions were prepared and analyzed by immunoblotting as described (16, 17). Real-time quantitative PCR was performed using gene-specific primers (Supplemental Table II).

Results

IEC-specific ablation of p38α expression results in colonic lymphoid hyperplasia

We previously generated and characterized mice with IEC-restricted p38α deficiency (designated p38αΔIEC). Their intestinal epithelium exhibited an imbalance in steady-state proliferation and differentiation: a dramatic increase in the former at the expense of the latter, which led to elongated epithelial lining of the villus and the crypt (8). It had remained unexplored, however, whether p38α signaling in IECs also serves noncell-autonomous functions, for example, related to the organization and maintenance of the nonepithelial compartments of the intestinal mucosa. Intriguingly, we found large increases in the absolute number of B cells and T cells in p38αΔIEC relative to wild-type (WT) colons (Fig. 1A). We performed histological analysis of colon tissue sections to determine whether these changes reflected increased numbers of diffuse lamina propria lymphocytes or increased cellularity in the follicular aggregates. Abnormal enlargement of ILFs was evident in p38αΔIEC colons at 12 wk of age (Fig. 1B, 1C). It is notable that, although the number of ILFs in the colon (i.e., colonic ILF density) increased in some p38αΔIEC mice, the overall difference between the WT and p38αΔIEC groups did not reach significance (Fig. 1D). The difference in ILF size, however, remained significant throughout life, with nearly all of p38αΔIEC mice exhibiting oversized ILFs (>300 μm in diameter) independently of their ILF numbers (Fig. 1D). Colonic ILF hyperplasia of this magnitude rarely developed among WT mice. Therefore, p38α signaling in IECs appeared to regulate the growth of committed ILFs, but not as critically the commitment of their formation per se. Peanut agglutinin staining showed that many but not all of overgrown ILFs in p38αΔIEC colons (four out of eight

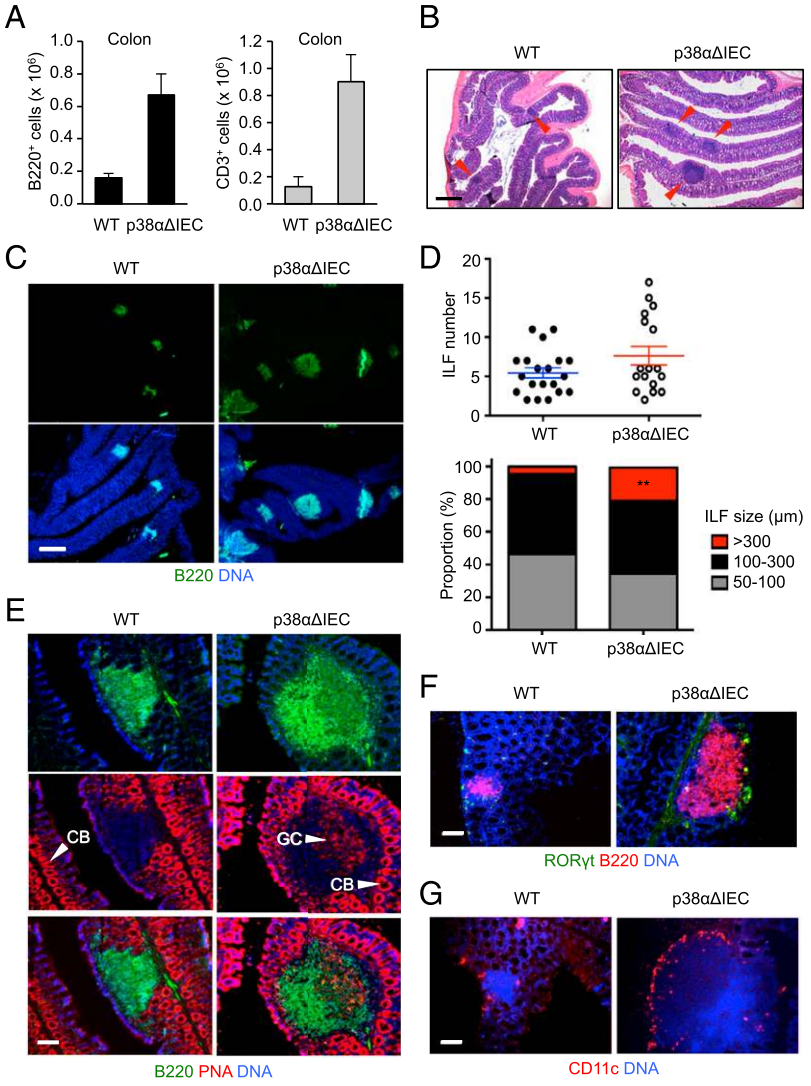

FIGURE 1. Mice lacking p38α in intestinal epithelial cells develop colonic lymphoid hyperplasia. Colon tissues were obtained from WT and p38αΔIEC mice at 12–16 wk of age. (**A**) The number of colonic B220$^+$ and CD3$^+$ cells was determined by flow cytometry, and is shown as mean ± SEM (n = 3). (**B** and **C**) Colon tissue sections were analyzed by H&E staining (B), and immunostaining for B220 together with counterstaining of DNA (C). Red arrowheads indicate ILFs. Scale bar, 500 μm (B and C). (**D**) The number of colonic ILFs (*upper panel*) and the proportions of their subsets grouped according to size (*lower panel*) were determined. $^{**}p < 0.005$. (**E**–**G**) Colon tissue sections were analyzed by peanut agglutinin staining and immunostaining for B220 (E), and immunostaining for RORγt and B220 (F), and CD11c (G) together with counterstaining of DNA. White arrowheads indicate germinal centers and the crypt base. Scale bar, 100 μm.

examined) had germinal centers, whereas there were few ILFs with germinal centers in WT colons (Fig. 1E).

In p38αΔIEC mice, RORγt$^+$ LTi/LTi-like cells and CD11c$^+$ dendritic cells were mainly distributed in areas overlaying the lymphoid follicle and proximal to the follicle-associated epithelium (Fig. 1F, 1G). This localization was normal, and suggested that the hyperplastic ILFs developing in p38αΔIEC colons retained the typical architecture of murine ILFs reported in earlier studies (18, 19).

We observed mild hyperplasia of Peyer's patches in some p38αΔIEC mice (Supplemental Fig. 1, A–C), yet these cases were episodic in nature and involved only minor changes in extent relative to the marked ILF hyperplasia seen in p38αΔIEC colons. Moreover, ILF hyperplasia was not detected in p38αΔIEC small intestines (Supplemental Fig. 1D). We therefore focused on colonic epithelial–lymphoid interactions for the remaining analysis of this study.

Colonic lymphoid hyperplasia resulting from IEC-specific p38α deficiency occurs independently of microbial stimuli

Loss of p38α in the intestinal epithelium might disrupt its barrier function and permit translocation of luminal bacteria and their products across the epithelial layer, a condition that could lead to immune activation and GALT hyperplasia. We investigated whether p38αΔIEC mice manifested evidence supporting this possibility, and first sought to assess their intestinal epithelial permeability. To this end, we traced fluorescently labeled dextran detected in the blood after its oral administration to WT and p38αΔIEC mice. The amounts of circulating dextran in the two groups were comparable (Fig. 2A), suggesting no difference in their barrier integrity. In addition, steady-state colons of p38αΔIEC mice did not exhibit elevated expression of tissue inflammation markers such as *Il1a*, *Il6*, *Cxcl1*, *Cxcl2*, and *Ptgs2* (Fig. 2B).

We next examined whether the occurrence of ILF hyperplasia in p38αΔIEC mice could be prevented or mitigated by depletion of the intestinal microbiota, which was indeed the case in some, but not all gene knockout mouse lines developing similar GALT hyperplasia (20–22). Long-term treatment with broad-spectrum antibiotics effectively depleted intestinal bacteria in WT and p38αΔIEC mice, as indicated by the fecal bacterial counts (Fig. 2C). The animals also displayed cecal enlargement (Fig. 2D), which is characteristic of germ-free and antibiotic-treated animals (23). Microbiota-depleted p38αΔIEC mice developed enlarged ILFs, as did antibiotic-naive p38αΔIEC mice (Fig. 2E). Although antibiotic treatment resulted in crypt hypotrophy in both WT and p38αΔIEC mice, the difference in ILF size persisted between the two groups of microbiota-depleted mice (Fig. 2E, 2F). These findings suggested that the development of colonic lymphoid hyperplasia in p38αΔIEC mice was independent of microbial stimuli and driven by more direct epithelial–lymphoid interactions. An

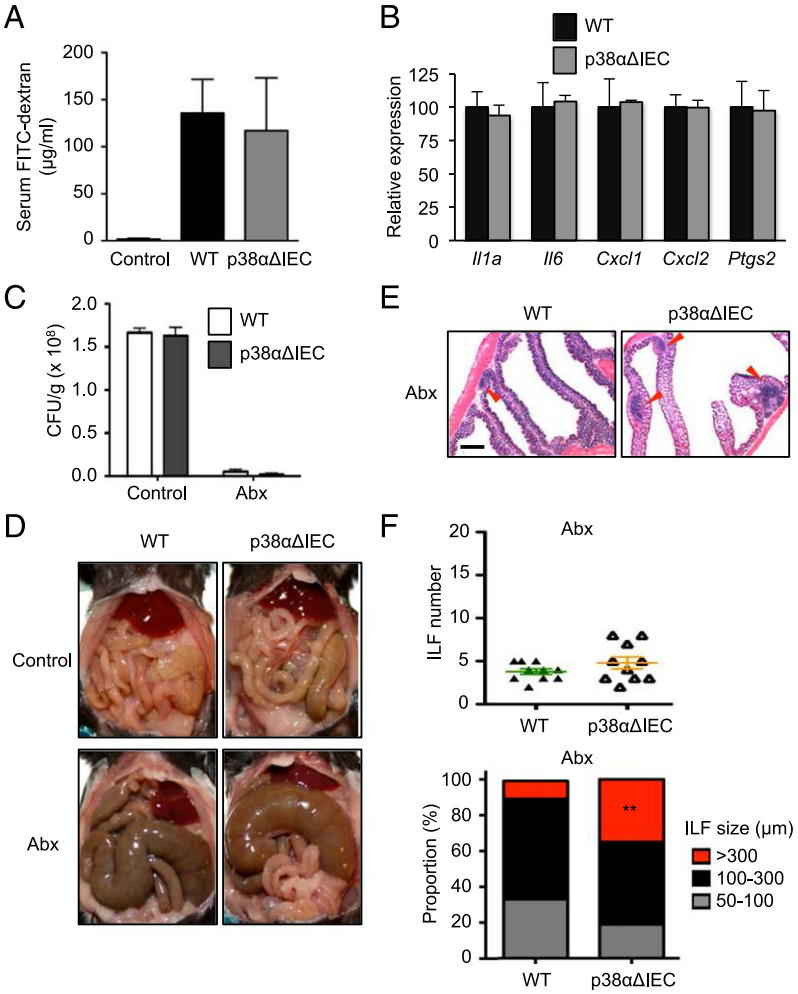

FIGURE 2. Epithelial p38α deficiency leads to colonic lymphoid hyperplasia independently of the influence of gut microbiota. (**A**) The concentration of FITC-dextran in serum of WT and p38αΔIEC mice was determined after its oral administration, and is shown as mean ± SEM (n = 3–4). (**B**) The expression of the indicated genes in the intestinal epithelium of WT and p38αΔIEC mice was analyzed by quantitative PCR. Data are shown as mean ± SEM. (**C**–**F**) WT and p38αΔIEC mice were subjected to long-term antibiotic treatment (Abx) and analyzed together with antibiotic-naive counterparts (Control). Fecal bacterial counts were determined (C). The abdominal viscera were photographed (D). Colon tissue sections were analyzed by H&E staining (E). Red arrowheads indicate ILFs. Scale bar, 500 μm. The number of colonic ILFs (F, *upper panel*) and the proportions of their subsets grouped according to size (F, *lower panel*) were determined. $^{**}p < 0.005$.

IEC-derived signal might, for instance, promote the recruitment or proliferation of lymphocytes comprising the ILF; such a signal might be excessively generated in p38α-deficient IECs.

IEC-specific ablation of p38α expression enhances colitis-associated lymphoid hyperplasia

Apart from steady-state GALT development, lymphoid neogenesis can occur in inflamed intestinal mucosa. Mild colitis induced by oral administration of low-dose (2.5%) DSS led to the growth of ILF-like structures in WT colons, but to a greater extent in p38αΔIEC colons (Fig. 3A). We reported that p38αΔIEC mice suffered severe IEC damage after, and eventually succumbed to, high-dose (3.5%) DSS administration (8). GALT hyperplasia in some mutant mouse lines has been associated with an increased severity of experimentally induced colitis (24, 25). The expanded lymphoid compartment in p38αΔIEC mice, however, seemed to contribute little to their susceptibility to DSS-induced colitis; p38αΔIEC mice in a RAG1-deficient background, hence devoid of GALT, showed mortality comparable to those of RAG1-sufficient counterparts upon high-dose DSS treatment (Fig. 3B).

IEC-specific ablation of p38α expression results in GALT malignancy

In an attempt to identify the long-term sequelae of deregulated GALT development in p38αΔIEC mice, we established groups of mice aged 48–72 wk. Macroscopically discernible nodules of overgrown ILFs and Peyer's patches emerged in these p38αΔIEC mice (Supplemental Fig. 2A). Furthermore, several aged p38αΔIEC mice had mesenteric lymph node hypertrophy and ectopic lymphoid neogenesis in periportal areas of the liver (Supplemental Fig. 2A–C), possibly indicating a propagation of GALT hyperplasia and aberrant homing of GALT-derived lymphocytes via the lymphatic and portal venous routes (26). GALT hypertrophy and hepatic lymphoid neogenesis were not observed in similarly aged WT mice.

Remarkably, lymphoid hyperplasia at intestinal and hepatic sites progressed to B cell lymphoma in some p38αΔIEC mice (Supplemental Fig. 2C, 2D). Malignant B cells disseminated to the bone marrow in these animals (Supplemental Fig. 2E). Analysis of the IgH gene rearrangement revealed monoclonality of lymphoma from each host, indicating that malignancies in p38αΔIEC mice arose from clonal expansion of transformed B cells (Supplemental Fig. 2F). Taken together, our findings with p38αΔIEC mice suggested that the intestinal epithelium provided critical signals for GALT development and homeostasis, dysregulation of which could lead to lymphoid hyperplasia and malignancy in the intestines and the liver. The generation of such signals seemed to be controlled by epithelial p38α signaling. We sought to identify this p38α-dependent regulatory mechanism operating in IECs.

NF-κB activation in IECs is restrained by p38α

We previously showed that genetic ablation or pharmacological inhibition of p38α resulted in enhanced phosphorylation and activation of TAK1 in various cell types (8). Given that TAK1 is required for NF-κB activation in a multitude of signaling contexts (27, 28), it seemed plausible that loss of p38α could augment NF-κB signaling

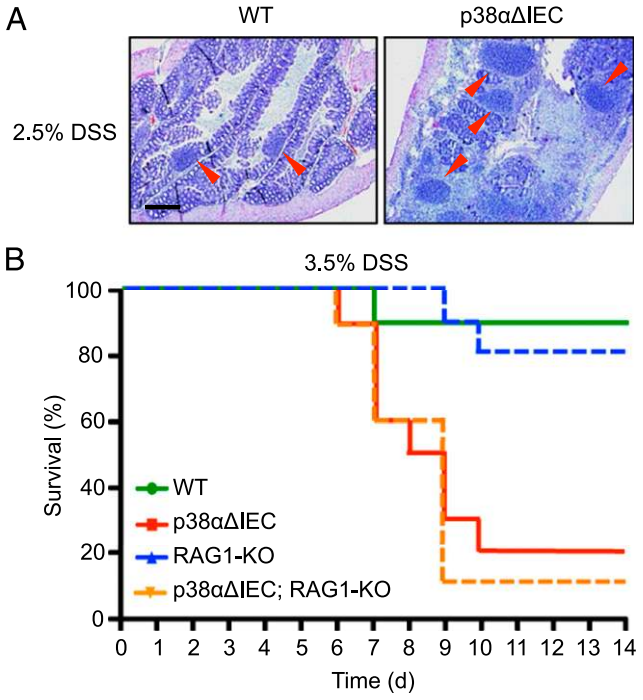

FIGURE 3. Colitis-associated lymphoid hyperplasia occurs to a greater extent in mice lacking p38α in intestinal epithelial cells. The indicated mice were administered DSS in drinking water at the indicated concentrations for 7 d. (**A**) Colon tissues were prepared on d 7 and analyzed by H&E staining. Red arrowheads indicate ILFs. Scale bar, 500 μm. (**B**) Survival was monitored daily (n = 10).

in IECs. To explore this idea, we first examined the effect of shRNA-mediated p38α gene knockdown (KD) on NF-κB activation, which is associated with the nuclear translocation of NF-κB RelA, in the immortalized mouse IEC line MODE-K. Of the six tested shRNA constructs with different target sequences, two (numbers 2 and 3) were effective at ablating p38α gene expression (Fig. 4A). MODE-K cells expressing shRNA from these constructs showed prolonged nuclear persistence of RelA upon TNF stimulation (Fig. 4B), an effect not observed with control constructs that either lacked a shRNA-encoding sequence (V) or expressed minimally effective shRNA (number 5).

Consistent with the reported role of p38α in TAK1 regulation, KD of p38α led to increases in basal as well as TNF-induced TAK1 phosphorylation in MODE-K cells (Fig. 4C, 4D). NF-κB induction in both control and p38α-KD cells was sensitive to the TAK1 inhibitor (5Z)-7-oxozeaenol (Fig. 4E). Of note, the rise of basal TAK1 activity in p38α-KD cells prior to TNF stimulation was not sufficient to activate NF-κB, suggesting that TAK1 hyperactivity in p38α-deficient cells is a prerequisite for enhanced NF-κB activation, yet should be accompanied by additional signaling events to affect it.

We next examined by immunofluorescence analysis the subcellular distribution of RelA in the colon tissue of WT and p38αΔIEC mice subjected to low-dose DSS (2.5%) administration (Fig. 4F). RelA signals were diffuse and mainly cytoplasmic throughout WT epithelium. By contrast, clusters of epithelial cells with intense signals of RelA concentrated in the nucleus were detected in p38αΔIEC colons. Therefore, our observations indicated that p38α served to restrain NF-κB activation in both cultured IECs and mouse colonic epithelium.

Enhanced NF-κB signaling in IECs results in GALT hyperplasia

Epithelial NF-κB signaling has been shown to play a key role in intestinal immune homeostasis and defense (29). In particular, NF-κB target gene expression in IECs has been found crucial for hematopoietic-derived cell recruitment to the lamina propria (12, 30). We therefore suspected that enhanced epithelial NF-κB signaling might be causally associated with increased GALT cellularity in p38αΔIEC mice. To address this possibility, we investigated mice expressing a constitutively active form of IKKβ (IKKβ^{EE}) in IECs and hence having IEC-restricted NF-κB hyperactivity (12). These mice (designated IEC-IKKβ^{EE}) displayed GALT hyperplasia similarly to p38αΔIEC mice (Fig. 5A, 5B). ILF numbers in IEC-IKKβ^{EE} colons increased moderately but not significantly compared with those in WT colon (Fig. 5C). IEC-IKKβ^{EE} mice, however, developed oversized colonic ILFs at a greatly increased rate as well as exhibiting an upward shift in the overall distribution of ILF sizes (Fig. 5C). GALT hyperplasia seen in p38αΔIEC mice and recapitulated in IEC-IKKβ^{EE} mice is therefore most likely attributable to enhanced NF-κB signaling in IECs. Unprovoked IEC-IKKβ^{EE} mice did not manifest an increased inflammatory tone in the intestinal mucosa; the expression of *Il1a*, *Il6*, *Cxcl1*, *Cxcl2*, and *Ptgs2* was comparable in steady-state intestines of WT and IEC-IKKβ^{EE} mice (Fig. 5D). Hence, the overgrowth of ILFs in IEC-IKKβ^{EE} mice did not seem secondary to inflammatory responses.

NF-κB–driven expression of GALT-related chemokines is regulated by p38α

A genome-wide expression analysis of the intestinal epithelium of IEC-IKKβ^{EE} mice identified numerous genes whose expression was elevated in IECs with constitutive NF-κB activation (12). Among these genes were *Ltb*, encoding the TNF family member lymphotoxin-β, and the chemokine genes *Ccl20* and *Cxcl16* (Fig. 6A). The contribution of lymphotoxin-β signaling to peripheral lymphoid tissue development is well established (10, 11). CCL20 and CXCL16, both expressed in the intestinal epithelium, have also been implicated in GALT formation in mice (31–34). By restraining NF-κB activation, p38α signaling might regulate the expression of these GALT-related NF-κB target genes in IECs. In keeping with this premise, *Ccl20* and *Cxcl16* expression was increased in the colonic epithelium of p38αΔIEC mice (Fig. 6B). In contrast, the expression of *Ltb* and other genes encoding GALT-related or IEC-derived cytokines (*Tnfsf13b*, *Il7*, *Tslp*, *Il25*, and *Il33*) and chemokines (*Cxcl13*) was comparable in WT and p38αΔIEC colons (Fig. 6B).

To investigate in greater detail how the IKKβ–NF-κB axis and p38α signaling interact to shape gene expression in IECs, we examined the effects of siRNA- and shRNA-mediated RelA and p38α gene KD (Figs. 6C, 4A, respectively) on the expression of TNF-inducible genes in MODE-K cells. The expression of a majority of TNF-inducible genes was abolished by RelA gene KD (Fig. 6D). TNF induction of a subset of the genes whose expression depended on RelA, including *Ccl20* and *Cxcl16*, was substantially enhanced by p38α gene KD (Fig. 6D, 6E). These results suggested that the regulatory function of p38α was directed toward specific NF-κB target genes in IECs. In summary, the changes in intracellular signaling and gene expression that we identified from p38α-deficient IECs were consistent with ILF hyperplasia in p38αΔIEC mice, and suggested CCL20 and CXCL16 as two possible mediators that link epithelial protein kinase signaling to GALT formation.

Discussion

We have identified a novel, noncell-autonomous role for p38α signaling in regulating GALT formation and maintenance. From an investigation of p38αΔIEC mice, we showed that genetic ablation of p38α signaling in IECs resulted in GALT hyperplasia,

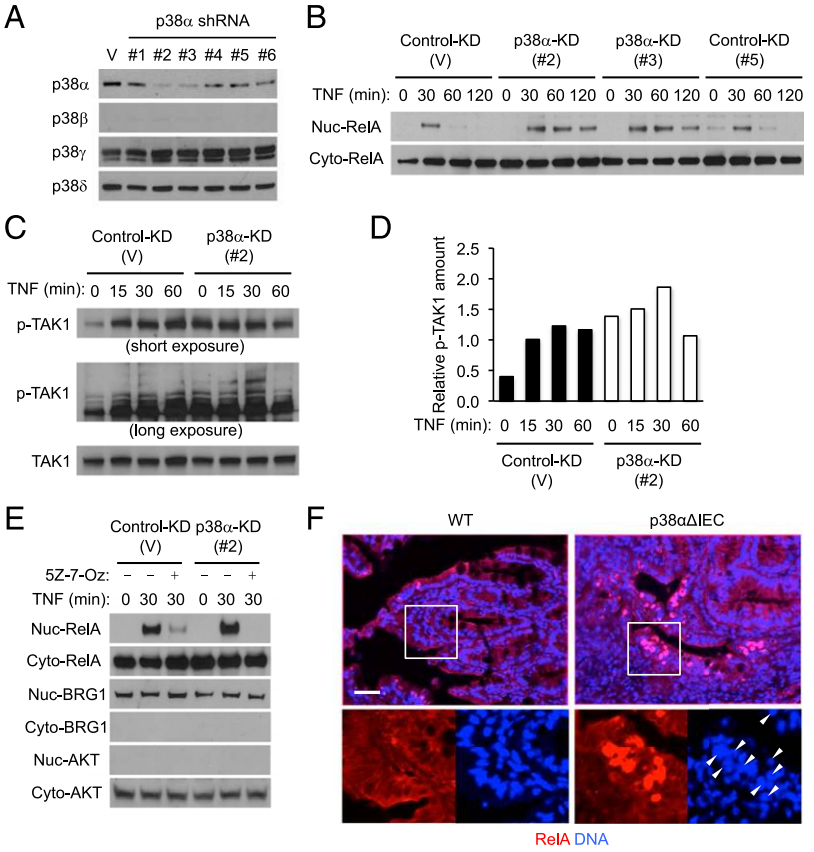

FIGURE 4. Intestinal epithelial cells lacking p38α exhibit NF-κB hyperactivation. (**A**) Whole-cell lysates were prepared from MODE-K cells expressing shRNA specific to p38α mRNA and control shRNA (V), and analyzed by immunoblotting. Numbers (1–6) denote shRNA clones with different target sequences. (**B**) Cytoplasmic (Cyto) and nuclear (Nuc) extracts were prepared from control (V and number 5) and p38α-KD (numbers 2 and 3) MODE-K cells at the indicated time points after treatment with TNF (50 ng/ml), and analyzed by immunoblotting. (**C** and **D**) Whole-cell lysates were prepared from control (V) and p38α-KD (number 2) MODE-K cells at the indicated time points after treatment with TNF (50 ng/ml), and analyzed by immunoblotting (C). The amount of phosphorylated (p-) TAK1 relative to that of total TAK1 was determined by densitometry (D). (**E**) Cytoplasmic and nuclear extracts were prepared and analyzed, as in (B). Where indicated, the cells were preincubated with the TAK1 inhibitor 5Z-7-Oz (2 μM) for 1 h before TNF exposure. (**F**) Colon tissues were prepared from WT and p38αΔIEC mice orally administered low-dose DSS (2.5%), as in Fig. 3, and analyzed by immunostaining for RelA with counterstaining of DNA. Arrowheads indicate nuclei with strong RelA signals. Scale bar, 100 μm.

which became more prominent as the animals aged and predisposed to B cell malignancy. Mechanistically, p38α attenuated TAK1–NF-κB signaling in IECs and thereby regulated epithelial expression of GALT-promoting chemokines. These findings illustrate that epithelial genetic alterations can cause or predispose to lymphoid hyperplasia and malignancy in mucosal tissues.

IEC-restricted loss of p38α signaling led to a striking increase in postnatal colonic ILF growth, but exerted lesser effects, if any, on prenatally developing GALT such as Peyer's patches. Both ILFs and Peyer's patches develop in a manner dependent on lymphotoxin-β receptor signaling and RORγ*t*-driven gene expression (18, 19, 35–37), yet the genetic requirements for their formation are not identical (38, 39). Epithelial p38α signaling presumably regulates a mechanism specifically linked to ILF development. This regulation does not likely involve the GALT-promoting effect of the intestinal microbiota, given that colonic ILF hyperplasia persisted in antibiotic-treated p38αΔIEC mice. It is noteworthy that, although luminal bacteria in general promote postnatal GALT development, several studies reported that colonic ILF development was not impeded in germ-free and antibiotic-treated

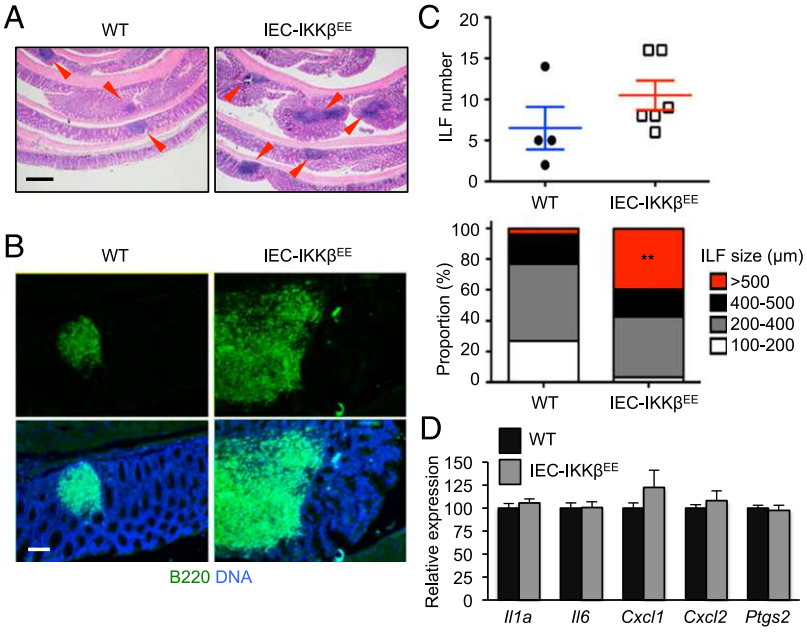

FIGURE 5. Mice with constitutive NF-κB activation in intestinal epithelial cells develop colonic lymphoid hyperplasia. Colon tissues were obtained from WT and IEC-IKKβ^{EE} mice at 35–45 wk of age. (**A** and **B**) Colon tissue sections were analyzed by H&E staining (A), and immunostaining for B220 together with counterstaining of DNA (B). Red arrowheads indicate ILFs. Scale bar, 500 μm (A) and 100 μm (B). (**C**) The number of colonic ILFs (*upper panel*) and the proportions of their subsets grouped according to size (*lower panel*) were determined. $^{**}p < 0.005$. (**D**) The expression of the indicated genes in the intestinal epithelium of WT and IEC-IKKβ^{EE} mice was analyzed by quantitative PCR. Data are shown as mean ± SEM.

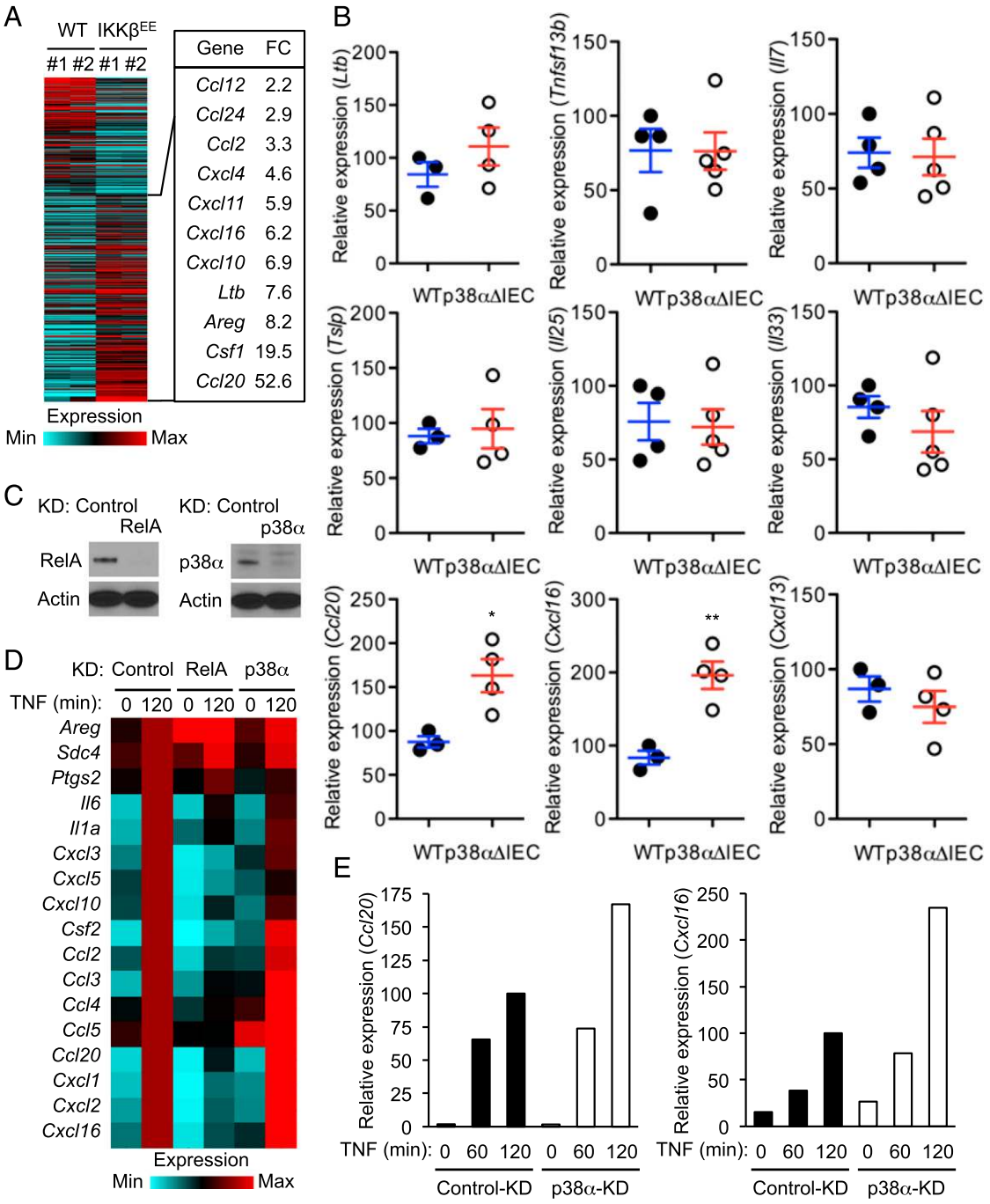

FIGURE 6. Loss of p38α augments NF-κB–driven chemokine gene expression in intestinal epithelial cells. (**A**) Intestinal epithelial cells from WT and IEC-IKKβ^{EE} mice (two animals for each genotype, numbers 1 and 2) were subjected to DNA microarray analysis. Relative RNA amounts for differentially expressed genes are presented in color-coded arbitrary units. Select genes showing higher expression in cells from IEC-IKKβ^{EE} mice relative to WT counterparts are indicated on the *right* along with the ratios (fold change [FC]) of their RNA amounts. (**B**) The expression of the indicated genes in the colonic epithelium of WT and p38αΔIEC mice was analyzed by quantitative PCR. Data for the colon are shown as mean ± SEM. (**C**–**E**) MODE-K cells were transfected with control and RelA- or p38α-specific siRNA (C and D), or with plasmids expressing control (V) and p38α-specific (number 2) shRNA (E). Whole-cell lysates were prepared and analyzed by immunoblotting (C). The expression of the indicated genes in TNF-treated cells was analyzed by quantitative PCR (D and E).

mice (33, 40–42). These findings indicate that the effects of intestinal microbiota are context dependent, and do not intervene in the p38α-mediated IEC–GALT interaction in the colon.

GALT hyperplasia in humans has been reported in association with pathological conditions of diverse etiologies (43, 44). Little information is available regarding the molecular mechanisms underlying the clinically observed GALT anomalies. Intriguingly, recent studies uncovered a link of some genetic alterations with specific cases. In particular, human subjects with germline mutations that result in phosphoinositide 3-kinase hyperactivation (e.g., *PTEN* loss-of-function, *PIK3CD* gain-of-function) have been found to develop nodular lymphoid hyperplasia in the small intestine and colon (45, 46). In addition, studies of mice with a targeted gene deletion or mutation have shown that GALT hyperplasia can arise from impaired Ig diversification or deregulated noncanonical NF-κB signaling (20, 47). The genetic alterations

investigated in these human and mouse studies led to an expansion of the B cell compartment in the GALT via cell-autonomous mechanisms, augmenting B cell proliferation, survival, or immune function. By contrast, our findings highlight the contribution of the epithelium as a niche to determining the size of B cell pools and other constituents of the GALT.

Loss of p38α signaling in IECs, while enhancing NF-κB activation, affected the expression of only a subset of NF-κB target genes, *Ccl20* and *Cxcl16* among others. Conceivably, additional signaling changes that paralleled NF-κB hyperactivation in p38α-deficient IECs (e.g., the loss of signaling downstream of p38α or the dysregulation of JNK or ERK signaling) might have an offsetting or overriding effect on NF-κB–driven gene expression; under such a circumstance, augmented NF-κB signaling in cells lacking p38α would not necessarily translate to an increase in global NF-κB target gene expression. We postulate that CCL20 and CXCL16 contribute to promoting GALT hyperplasia and malignancy in p38αΔIEC mice, yet do not exclude possible involvement of other gene products. CCR6 and CXCR6, the receptors for CCL20 and CXCL16, respectively, are expressed in ILF B cells (32) and LTi cells (48–51). Of note, it has been reported that CCR6 and CXCR6 are also highly expressed in clinical specimens of mucosa-associated B cell lymphoma, and that the epithelium neighboring the lymphoma expresses CCL20 (52, 53). The precise roles of the two chemokines in GALT and B cell homeostasis remain to be scrutinized. Further investigation of epithelial–lymphoid interactions in p38αΔIEC and IEC-IKKβ^{EE} mice may reveal novel IEC-derived molecular signals that produce various lymphoid tissue abnormalities in the intestinal mucosa.

Acknowledgments

We thank Ila Joshi and Katia Georgopoulos for technical advice on the analysis of Ig gene rearrangement and germinal centers.

Disclosures

The authors have no financial conflicts of interest.

References

1. Brewster, J. L., and M. C. Gustin. 2014. Hog1: 20 years of discovery and impact. *Sci. Signal.* 7: re7.
2. Trempolec, N., N. Dave-Coll, and A. R. Nebreda. 2013. SnapShot: p38 MAPK signaling. *Cell* 152: 656–656.e1.
3. Gupta, J., and A. R. Nebreda. 2015. Roles of p38α mitogen-activated protein kinase in mouse models of inflammatory diseases and cancer. *FEBS J.* 282: 1841–1857.
4. Hui, L., L. Bakiri, A. Mairhorfer, N. Schweifer, C. Haslinger, L. Kenner, V. Komnenovic, H. Scheuch, H. Beug, and E. F. Wagner. 2007. p38α suppresses normal and cancer cell proliferation by antagonizing the JNK-c-Jun pathway. *Nat. Genet.* 39: 741–749.
5. Ventura, J. J., S. Tenbaum, E. Perdiguero, M. Huth, C. Guerra, M. Barbacid, M. Pasparakis, and A. R. Nebreda. 2007. p38α MAP kinase is essential in lung stem and progenitor cell proliferation and differentiation. *Nat. Genet.* 39: 750–758.
6. Sakurai, T., G. He, A. Matsuzawa, G. Y. Yu, S. Maeda, G. Hardiman, and M. Karin. 2008. Hepatocyte necrosis induced by oxidative stress and IL-1α release mediate carcinogen-induced compensatory proliferation and liver tumorigenesis. *Cancer Cell* 14: 156–165.
7. Otsuka, M., Y. J. Kang, J. Ren, H. Jiang, Y. Wang, M. Omata, and J. Han. 2010. Distinct effects of p38α deletion in myeloid lineage and gut epithelia in mouse models of inflammatory bowel disease. *Gastroenterology* 138: 1255–1265, 1265.e1–1265.e9.
8. Caballero-Franco, C., M. K. Choo, Y. Sano, P. Ritprajak, H. Sakurai, K. Otsu, A. Mizoguchi, and J. M. Park. 2013. Tuning of protein kinase circuitry by p38α is vital for epithelial tissue homeostasis. *J. Biol. Chem.* 288: 23788–23797.
9. Gupta, J., I. del Barco Barrantes, A. Igea, S. Sakellariou, I. S. Pateras, V. G. Gorgoulis, and A. R. Nebreda. 2014. Dual function of p38α MAPK in colon cancer: suppression of colitis-associated tumor initiation but requirement for cancer cell survival. *Cancer Cell* 25: 484–500.
10. Pearson, C., H. H. Uhlig, and F. Powrie. 2012. Lymphoid microenvironments and innate lymphoid cells in the gut. *Trends Immunol.* 33: 289–296.
11. Randall, T. D., and R. E. Mebius. 2014. The development and function of mucosal lymphoid tissues: a balancing act with micro-organisms. *Mucosal Immunol.* 7: 455–466.
12. Guma, M., D. Stepniak, H. Shaked, M. E. Spehlmann, S. Shenouda, H. Cheroutre, I. Vicente-Suarez, L. Eckmann, M. F. Kagnoff, and M. Karin. 2011. Constitutive intestinal NF-κB does not trigger destructive inflammation unless accompanied by MAPK activation. *J. Exp. Med.* 208: 1889–1900.
13. Vidal, K., I. Grosjean, J. P. evillard, C. Gespach, and D. Kaiserlian. 1993. Immortalization of mouse intestinal epithelial cells by the SV40-large T gene: phenotypic and immune characterization of the MODE-K cell line. *J. Immunol. Methods* 166: 63–73.
14. Shimomura, Y., A. Ogawa, M. Kawada, K. Sugimoto, E. Mizoguchi, H. N. Shi, S. Pillai, A. K. Bhan, and A. Mizoguchi. 2008. A unique B2 B cell subset in the intestine. *J. Exp. Med.* 205: 1343–1355.
15. Fuxa, M., J. Skok, A. Souabni, G. Salvagiotto, E. Roldan, and M. Busslinger. 2004. Pax5 induces V-to-DJ rearrangements and locus contraction of the immunoglobulin heavy-chain gene. *Genes Dev.* 18: 411–422.
16. Park, J. M., V. H. Ng, S. Maeda, R. F. Rest, and M. Karin. 2004. Anthrolysin O and other Gram-positive cytolysins are Toll-like receptor 4 agonists. *J. Exp. Med.* 200: 1647–1655.
17. Enzler, T., Y. Sano, M. K. Choo, H. B. Cottam, M. Karin, H. Tsao, and J. M. Park. 2011. Cell-selective inhibition of NF-κB signaling improves therapeutic index in a melanoma chemotherapy model. *Cancer Discov.* 1: 496–507.
18. Hamada, H., T. Hiroi, Y. Nishiyama, H. Takahashi, Y. Masunaga, S. Hachimura, S. Kaminogawa, H. Takahashi-Iwanaga, T. Iwanaga, H. Kiyono, et al. 2002. Identification of multiple isolated lymphoid follicles on the antimesenteric wall of the mouse small intestine. *J. Immunol.* 168: 57–64.
19. Tsuji, M., K. Suzuki, H. Kitamura, M. Maruya, K. Kinoshita, I. I. Ivanov, K. Itoh, D. R. Littman, and S. Fagarasan. 2008. Requirement for lymphoid tissue-inducer cells in isolated follicle formation and T cell-independent immunoglobulin A generation in the gut. *Immunity* 29: 261–271.
20. Fagarasan, S., M. Muramatsu, K. Suzuki, H. Nagaoka, H. Hiai, and T. Honjo. 2002. Critical roles of activation-induced cytidine deaminase in the homeostasis of gut flora. *Science* 298: 1424–1427.
21. Pabst, O., H. Herbrand, M. Friedrichsen, S. Velaga, M. Dorsch, G. Berhardt, T. Worbs, A. J. Macpherson, and R. Förster. 2006. Adaptation of solitary intestinal lymphoid tissue in response to microbiota and chemokine receptor CCR7 signaling. *J. Immunol.* 177: 6824–6832.
22. Lochner, M., C. Ohnmacht, L. Presley, P. Bruhns, M. Si-Tahar, S. Sawa, and G. Eberl. 2011. Microbiota-induced tertiary lymphoid tissues aggravate inflammatory disease in the absence of RORgamma t and LTi cells. *J. Exp. Med.* 208: 125–134.
23. Savage, D. C., and R. Dubos. 1968. Alterations in the mouse cecum and its flora produced by antibacterial drugs. *J. Exp. Med.* 128: 97–110.
24. Olson, T. S., G. Bamias, M. Naganuma, J. Rivera-Nieves, T. L. Burcin, W. Ross, M. A. Morris, T. T. Pizarro, P. B. Ernst, F. Cominelli, and K. Ley. 2004. Expanded B cell population blocks regulatory T cells and exacerbates ileitis in a murine model of Crohn disease. *J. Clin. Invest.* 114: 389–398.
25. Kawamura, T., T. Kanai, T. Dohi, K. Uraushihara, T. Totsuka, R. Iiyama, C. Taneda, M. Yamazaki, T. Nakamura, T. Higuchi, et al. 2004. Ectopic CD40 ligand expression on B cells triggers intestinal inflammation. *J. Immunol.* 172: 6388–6397.
26. Adams, D. H., and B. Eksteen. 2006. Aberrant homing of mucosal T cells and extra-intestinal manifestations of inflammatory bowel disease. *Nat. Rev. Immunol.* 6: 244–251.
27. Wang, C., L. Deng, M. Hong, G. R. Akkaraju, J. Inoue, and Z. J. Chen. 2001. TAK1 is a ubiquitin-dependent kinase of MKK and IKK. *Nature* 412: 346–351.
28. Shim, J. H., C. Xiao, A. E. Paschal, S. T. Bailey, P. Rao, M. S. Hayden, K. Y. Lee, C. Bussey, M. Steckel, N. Tanaka, et al. 2005. TAK1, but not TAB1 or TAB2, plays an essential role in multiple signaling pathways in vivo. *Genes Dev.* 19: 2668–2681.
29. Pasparakis, M. 2012. Role of NF-κB in epithelial biology. *Immunol. Rev.* 246: 346–358.
30. Vlantis, K., A. Wullaert, Y. Sasaki, M. Schmidt-Supprian, K. Rajewsky, T. Roskams, and M. Pasparakis. 2011. Constitutive IKK2 activation in intestinal epithelial cells induces intestinal tumors in mice. *J. Clin. Invest.* 121: 2781–2793.
31. Hase, K., T. Murakami, H. Takatsu, T. Shimaoka, M. Iimura, K. Hamura, K. Kawano, S. Ohshima, R. Chihara, K. Itoh, et al. 2006. The membrane-bound chemokine CXCL16 expressed on follicle-associated epithelium and M cells mediates lympho-epithelial interaction in GALT. *J. Immunol.* 176: 43–51.
32. McDonald, K. G., J. S. McDonough, C. Wang, T. Kucharzik, I. R. Williams, and R. D. Newberry. 2007. CC chemokine receptor 6 expression by B lymphocytes is essential for the development of isolated lymphoid follicles. *Am. J. Pathol.* 170: 1229–1240.
33. Bouskra, D., C. Brézillon, M. Bérard, C. Werts, R. Varona, I. G. Boneca, and G. Eberl. 2008. Lymphoid tissue genesis induced by commensals through NOD1 regulates intestinal homeostasis. *Nature* 456: 507–510.
34. Obata, Y., S. Kimura, G. Nakato, K. Iizuka, Y. Miyagawa, Y. Nakamura, Y. Furusawa, M. Sugiyama, K. Suzuki, M. Ebisawa, et al. 2014. Epithelial-stromal interaction via Notch signaling is essential for the full maturation of gut-associated lymphoid tissues. *EMBO Rep.* 15: 1297–1304.
35. De Togni, P., J. Goellner, N. H. Ruddle, P. R. Streeter, A. Fick, S. Mariathasan, S. C. Smith, R. Carlson, L. P. Shornick, J. Strauss-Schoenberger, et al. 1994. Abnormal development of peripheral lymphoid organs in mice deficient in lymphotoxin. *Science* 264: 703–707.
36. Lorenz, R. G., D. D. Chaplin, K. G. McDonald, J. S. McDonough, and R. D. Newberry. 2003. Isolated lymphoid follicle formation is inducible and dependent upon lymphotoxin-sufficient B lymphocytes, lymphotoxin β receptor, and TNF receptor I function. *J. Immunol.* 170: 5475–5482.

37. Eberl, G., S. Marmon, M. J. Sunshine, P. D. Rennert, Y. Choi, and D. R. Littman. 2004. An essential function for the nuclear receptor RORgamma(t) in the generation of fetal lymphoid tissue inducer cells. *Nat. Immunol.* 5: 64–73.
38. Knoop, K. A., B. R. Butler, N. Kumar, R. D. Newberry, and I. R. Williams. 2011. Distinct developmental requirements for isolated lymphoid follicle formation in the small and large intestine: RANKL is essential only in the small intestine. *Am. J. Pathol.* 179: 1861–1871.
39. Lee, J. S., M. Cella, K. G. McDonald, C. Garlanda, G. D. Kennedy, M. Nukaya, A. Mantovani, R. Kopan, C. A. Bradfield, R. D. Newberry, and M. Colonna. 2012. AHR drives the development of gut ILC22 cells and postnatal lymphoid tissues via pathways dependent on and independent of Notch. *Nat. Immunol.* 13: 144–151.
40. Kweon, M. N., M. Yamamoto, P. D. Rennert, E. J. Park, A. Y. Lee, S. Y. Chang, T. Hiroi, M. Nanno, and H. Kiyono. 2005. Prenatal blockage of lymphotoxin beta receptor and TNF receptor p55 signaling cascade resulted in the acceleration of tissue genesis for isolated lymphoid follicles in the large intestine. *J. Immunol.* 174: 4365–4372.
41. Baptista, A. P., B. J. Olivier, G. Goverse, M. Greuter, M. Knippenberg, K. Kusser, R. G. Domingues, H. Veiga-Fernandes, A. D. Luster, A. Lugering, et al. 2013. Colonic patch and colonic SILT development are independent and differentially regulated events. *Mucosal Immunol.* 6: 511–521.
42. Donaldson, D. S., B. M. Bradford, D. Artis, and N. A. Mabbott. 2015. Reciprocal regulation of lymphoid tissue development in the large intestine by IL-25 and IL-23. *Mucosal Immunol.* 8: 582–595.
43. Mansueto, P., G. Iacono, A. Seidita, A. D'Alcamo, D. Sprini, and A. Carroccio. 2012. Review article: intestinal lymphoid nodular hyperplasia in children–the relationship to food hypersensitivity. *Aliment. Pharmacol. Ther.* 35: 1000–1009.
44. Albuquerque, A. 2014. Nodular lymphoid hyperplasia in the gastrointestinal tract in adult patients: a review. *World J. Gastrointest. Endosc.* 6: 534–540.
45. Heindl, M., N. Händel, J. Ngeow, J. Kionke, C. Wittekind, M. Kamprad, A. Rensing-Ehl, S. Ehl, J. Reifenberger, C. Loddenkemper, et al. 2012. Autoimmunity, intestinal lymphoid hyperplasia, and defects in mucosal B-cell homeostasis in patients with PTEN hamartoma tumor syndrome. *Gastroenterology* 142: 1093–1096.e6.
46. Lucas, C. L., H. S. Kuehn, F. Zhao, J. E. Niemela, E. K. Deenick, U. Palendira, D. T. Avery, L. Moens, J. L. Cannons, M. Biancalana, et al. 2014. Dominant-activating germline mutations in the gene encoding the PI(3)K catalytic subunit p110δ result in T cell senescence and human immunodeficiency. *Nat. Immunol.* 15: 88–97.
47. Conze, D. B., Y. Zhao, and J. D. Ashwell. 2010. Non-canonical NF-κB activation and abnormal B cell accumulation in mice expressing ubiquitin protein ligase-inactive c-IAP2. *PLoS Biol.* 8: e1000518.
48. Lügering, A., M. Ross, M. Sieker, J. Heidemann, I. R. Williams, W. Domschke, and T. Kucharzik. 2010. CCR6 identifies lymphoid tissue inducer cells within cryptopatches. *Clin. Exp. Immunol.* 160: 440–449.
49. Sawa, S., M. Cherrier, M. Lochner, N. Satoh-Takayama, H. J. Fehling, F. Langa, J. P. Di Santo, and G. Eberl. 2010. Lineage relationship analysis of RORgammat^{+} innate lymphoid cells. *Science* 330: 665–669.
50. Possot, C., S. Schmutz, S. Chea, L. Boucontet, A. Louise, A. Cumano, and R. Golub. 2011. Notch signaling is necessary for adult, but not fetal, development of RORγt($^{+}$) innate lymphoid cells. *Nat. Immunol.* 12: 949–958.
51. Satoh-Takayama, N., N. Serafini, T. Verrier, A. Rekiki, J. C. Renauld, G. Frankel, and J. P. Di Santo. 2014. The chemokine receptor CXCR6 controls the functional topography of interleukin-22 producing intestinal innate lymphoid cells. *Immunity* 41: 776–788.
52. Rodig, S. J., D. Jones, A. Shahsafaei, and D. M. Dorfman. 2002. CCR6 is a functional chemokine receptor that serves to identify select B-cell non-Hodgkin's lymphomas. *Hum. Pathol.* 33: 1227–1233.
53. Deutsch, A. J., E. Steinbauer, N. A. Hofmann, D. Strunk, T. Gerlza, C. Beham-Schmid, H. Schaider, and P. Neumeister. 2013. Chemokine receptors in gastric MALT lymphoma: loss of CXCR4 and upregulation of CXCR7 is associated with progression to diffuse large B-cell lymphoma. *Mod. Pathol.* 26: 182–194.